

Received:
17 March 2020Revised:
08 July 2020Accepted:
09 July 2020<https://doi.org/10.1259/bjr.20200257>

Cite this article as:

Saleh MM, Abdelrahman TM, Madney Y, Mohamed G, Shokry AM, Moustafa AF. Multiparametric MRI with diffusion-weighted imaging in predicting response to chemotherapy in cases of osteosarcoma and Ewing's sarcoma. *Br J Radiol* 2020; **93**: 20200257.

FULL PAPER

Multiparametric MRI with diffusion-weighted imaging in predicting response to chemotherapy in cases of osteosarcoma and Ewing's sarcoma

¹MAHMOUD MOHAMED SALEH, ¹TAMER MOUSTAFA ABDELRAHMAN, ²YOUUSEF MADNEY, ³GHADA MOHAMED, ¹AHMED MOHAMMED SHOKRY and ¹AMR FAROUK MOUSTAFA, PhD¹Department of diagnostic and interventional radiology, National Cancer Institute, Cairo University, Cairo, Egypt²Department of pediatric oncology, National Cancer Institute, Cairo University, Cairo, Egypt³Department of surgical pathology, National Cancer Institute, Cairo University, Cairo, EgyptAddress correspondence to: Dr Amr Farouk Moustafa
E-mail: amrfaroukmoustafa@cu.edu.eg

Objective: To evaluate the multiparametric MRI in predicting chemotherapy response in pathologically proven cases of osteosarcoma and Ewing's sarcoma. Correlation between the tumor size changes and internal breakdown using RECIST 1.1, modified RECIST, quantitative apparent diffusion coefficient (ADC) and tumor volume as well as dynamic contrast-enhanced MRI (DCE-MRI).

Methods: The study included 104 patients pathologically proved osteosarcoma (53) and Ewing's sarcoma (51) underwent MRI examinations; before and after chemotherapy. All patients were assessed using the RECIST 1.1 criteria, m-RECIST, quantitative ADC, and tumor volume evaluation. 21 patients underwent DCE-MRI curve type with quantitative parameters. Correlation between the different evaluations was carried out. Results were correlated with the post-operative pathology in 42 patients who underwent surgery and for statistical evaluation, Those patients were classified into responders ($\geq 90\%$ necrosis) and non-responders ($< 90\%$ necrosis).

Results: The initial mean ADC of 104 patients of osteosarcoma and Ewing's sarcoma (0.90 ± 0.29) and (0.71 ± 0.16) respectively, differed significantly from that after treatment (1.62 ± 0.46) and (1.6 ± 0.39) respectively with ($p < 0.001$).

ADC variations (ADC%) in the non-progressive group were higher than those of the progressive group (128.3 ± 63.49 vs 36.34 ± 78.7) % with ($p < 0.001$).

ADC values and ADC variations were inversely correlated with morphologic changes, regardless of the effectiveness of chemotherapy expressed as changes in tumor size based on (RECIST 1.1, RECIST, and 3D volume). Linear regression analysis revealed a Pearson correlation coefficient of $r = -0.427$, -0.498 and -0.408 , respectively with ($p < 0.001$).

An increase in the ADC value was not always associated with a reduction in tumor volume. The disease control rate (defined as the percentage of CR+PR+SD patients) was 89.4% and 93.9% according to RECIST 1.1 and m-RECIST respectively.

42 out of the 104 patients had postsurgical histological evaluation as regards the chemotherapeutic response divided into two groups. ADC values showed a statistically significant difference between Group A and Group B being more evident with minimum ADC% ($p < 0.001$).

Conclusion: Quantitative diffusion-weighted imaging with ADC mapping and ADC % after chemotherapy allows a detailed analysis of the treatment response in osteosarcoma and Ewing's sarcoma. The therapeutic response can be underestimated using RECIST 1.1, so the modified RECIST should be also considered.

Advances in knowledge: Quantitative ADC especially ADC% provided an accurate non-invasive tool in the assessment of post-therapeutic cases of osteosarcoma and Ewing's sarcoma

INTRODUCTION

Osteosarcoma is the most common malignant bone tumor in adolescents and young adults followed by Ewing sarcoma (ES) in second place.¹

Primary osteosarcoma has different types and subtypes, including intramedullary (conventional, high grade, low grade, telangiectatic, small cell, osteosarcomatosis, and gnathic), surface (intracortical, parosteal, periosteal, and high-grade surface), and extra skeletal. osteosarcoma may

also occur as a secondary lesion in association with underlying benign conditions.²

ES family of tumors includes osseous ES, extra skeletal ES, primitive neuroectodermal tumor, and Askin's tumor.³

Traditional treatment of these malignant bone tumors consists of neoadjuvant chemotherapy before definitive surgical resection with early-stage tumors or adjuvant chemoradiotherapy in non-surgical candidate patients.¹ A vital component of management involves the assessment of treatment response to chemotherapy to predict the patient's prognosis.⁴

MRI is now the most commonly used non-invasive modality includes anatomical and functional assessment by fluid sensitive and post-contrast imaging sequences.⁵

Post-treatment evaluation using functional MR imaging sequences adds value after chemotherapy and/or radiation therapy to help determine treatment response and distinguish post-operative fibrosis and inflammation/necrosis.⁶

Diffusion-weighted imaging (DWI) of musculoskeletal lesions has shown promising results in therapy surveillance of primary malignant bone tumors. Furthermore, it has also been demonstrated to be cost-effective by limiting or eliminating the need for further diagnostic tests or surgical procedures.⁴

This study aimed to assess the diagnostic merits of dynamic contrast-enhanced (DCE)-MR imaging and DWI with ADC mapping in initially diagnosed cases of osteosarcoma and ES, determine quantitative mean ADC values of these tumors, and the possibility of use of DWI to assess treatment response in

correlation with different systems of standardized reporting used for categorizing the therapeutic response of cancer patients.

METHODS AND MATERIALS

Patients

This prospective study included 104 patients, their ages range from 2 to 49 years with a median age of 19 years. Mean age 20 ± 10.5 years. The study has been approved by the "Ethical Committee of the national cancer institute, Cairo University, Egypt", in compliance with the Helsinki Declaration.

Patients included were patients referred to the radiology department who are diagnosed with pathologically proven osteosarcoma or Ewing's sarcoma. Initial MRI assessment before treatment followed by neoadjuvant or adjuvant chemotherapy and/or radiotherapy then a follow-up MRI was carried out.

Patients excluded were patients having chemotherapy and/or radiotherapy before initial MRI as well as the absolute contraindications for MRI examination, including contraindication to contrast media.

Magnetic resonance imaging

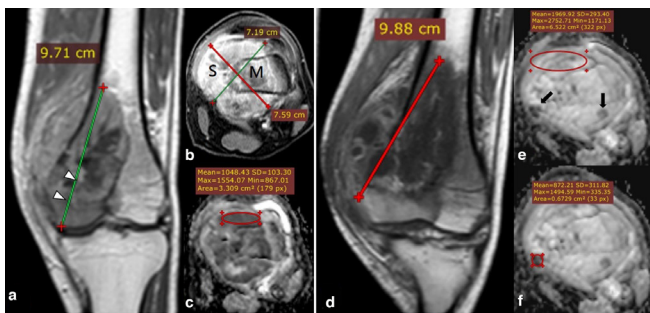
The patients had their MRI done on a high field system (1.5 T) closed magnet unit (Phillips Achieva XR). The MRI technique included:-

- Multiplanar MR imaging sequences without contrast including T_1 and T_2 WI.
- Gadolinium-enhanced T_1 weighted sequences.
- Diffusion-weighted sequence with four b-values (b=0, 50, 400 and 800).

Table 1. Initial pathology and tumor locations included in this study

Initial pathology		Count	Percentage (%)	Total Count (%)
Ewing's sarcoma/PENT		53	51.0	104 (100%)
Osteosarcoma		51	49.0	
Osteosarcoma subtypes	Conventional osteosarcoma	41	80	51 (100%)
	Telengectatic osteosarcoma	5	10	
	Chondrolastic osteosarcoma	1	2	
	Osteoblastoma like variant osteosarcoma	1	2	
	Osteosarcoma small cell	1	2	
	Parosteal osteosarcoma	2	4	
Tumor location				
Skeletal tumors	Extremities	60	57.7	92 (88.5%)
	Axial skeleton	32	30.8	
Extra skeletal tumors		12	11.5	12 (11.5%)
Total				104 (100%)

Figure 1. 19-year-old male with right femoral bone osteosarcoma conventional type (initial MRI assessment). Post-contrast coronal T1 (A), axial T1-fat sat. (B) showing right distal femoral metaphysis heterogeneous enhancing marrow lesion (m) with lateral cortical breaching (Arrowheads) and eccentric extra osseous soft tissue component (s), with a calculated volume of 276 CC. ADC map (C) showing restricted low signal intensity compared to the nearby normal muscles with ADC values of (mean: $1 \times 10^{-3} \text{ mm}^2/\text{s}$ and minimum: $0.8 \times 10^{-3} \text{ mm}^2/\text{s}$). Follow-up MRI after 6 months with post-contrast coronal T1 (D) showing increased dimensions and volume of the previously noted right femoral lesion with a calculated volume of 315 CC. Yet volume% and RECIST suggest stable disease (changes less than 20% increased in size). Follow-up ADC mapping (E, F) show predominantly facilitated signal (ROI with a value of mean $1.9 \times 10^{-3} \text{ mm}^2/\text{s}$ and minimum $1.2 \times 10^{-3} \text{ mm}^2/\text{s}$) with internal foci of restricted signal marked by "Black arrows" (targeted ROI is placed with values of mean $0.8 \times 10^{-3} \text{ mm}^2/\text{s}$ and minimum $0.4 \times 10^{-3} \text{ mm}^2/\text{s}$). The post-operative histopathological assessment revealed about 20% tumoral viability within the lesion denoting poor therapeutic response, which matches the DWI and ADC mapping despite stable disease as regards the size (RESIST and Vol.% change). ADC, apparent diffusion coefficient; ROI, region of interest.



- ADC maps were calculated from the diffusion-weighted images.
- Gadolinium-enhanced T_1 weighted sequences with DCE images done in some of the cases with qualitative time-intensity curve assessment.
- The MRI protocols were tailored according to the site of the lesion including the used coil and imaging plans.

Follow-up of treatment

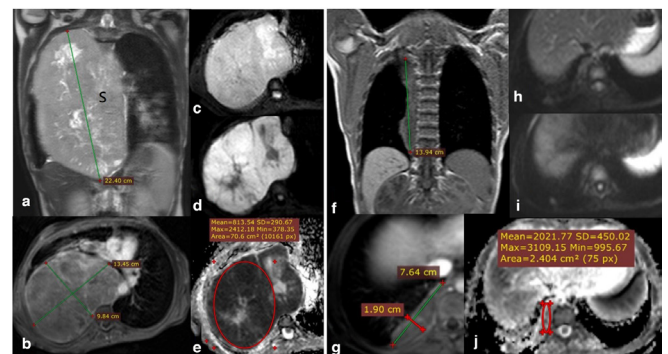
Follow-up MR examinations of average 3–6 months after chemotherapy administration. These patients had different management plans including two groups of chemotherapy: (Vincristine, Doxorubicin, and Cyclophosphamide) and (Etoposide and Ifosfamide).

For those lesions, follow-up examination were evaluated and documented to assess the response to treatment. This was carried out by evaluating the changes in tumor size, breakdown, and ADC calculations.

Image analysis

- The morphological MRI features including site, extensions, signal characteristics, and pattern of enhancement.

Figure 2. 14-year-old male presented with thoraco-pulmonary extra skeletal Ewing's sarcoma. Coronal STIR WI (A) and axial post-contrast T1 fat saturation (B) showing huge right hemithoracic heterogeneously avid enhancing soft tissue mass lesion (s) with intrinsic areas of cystic changes/breakdown, the calculated volume of 1990 CC. DWI (b0 and b-800) images (C) & (D) show bright signal in highest b value and corresponding low signal in ADC map (E) with calculated ADC values of (mean: $0.81 \times 10^{-3} \text{ mm}^2/\text{s}$ and minimum: $0.37 \times 10^{-3} \text{ mm}^2/\text{s}$). Follow-up MRI study after 6 months of chemotherapy: post-contrast coronal T1 (F), Post-contrast axial T1 fat saturation (G) showing notable regression as regards the size and calculated volume of the right thoracic lesion with a calculated volume of 108.4 CC. DWI (b0 and b-800) images (H, I) as well as ADC map (J) showing facilitation of signal intensity with ADC values (mean: $2.0 \times 10^{-3} \text{ mm}^2/\text{s}$ and minimum: $1 \times 10^{-3} \text{ mm}^2/\text{s}$). Denoting good therapeutic response matching the regressive response of the RESIST and vol.% change. ADC, apparent diffusion coefficient; DWI, diffusion-weighted imaging.



- Other morphological features including:

- Tumor longest dimension according to RECIST 1.1,
- The longest dimension of the contrast-enhanced portion of the tumor according to (m-RECIST),
- And, the tumor volume (VOL) expressed in cubic centimeters (ccm) was assessed according to the following equation:

$$VOL = [X \times Y \times Z] \times F$$

Where X , Y , and Z represents the longest three dimensions, $F = \frac{\pi}{4}$ in cylindrical lesions and $F = \frac{\pi}{6}$ in ellipsoid lesions.

-Finally, we reviewed the diffusion images with ADC values.

All these criteria were independently reviewed by two experienced radiologists for the documentation of these findings.

Interpretation of diffusion-weighted images and ADC calculation:

- 102 out of 104 patients underwent DWI and ADC mapping with quantitative ADC values. The excluded two patients had technical limitations in the acquisition of the DWIs including motion artifact in chest wall and improper coil usage.

Table 2. Detailed analysis of tumor volumes before and after neoadjuvant treatment in the progressive and non-progressive group and both groups together with volume variation % changes

Volume groups	Progressive disease group (11 cases)					Non-progressive disease group (93 cases)					Both groups	
	Mean	SD	Median	Minimum	Maximum	Mean	SD	Median	Minimum	Maximum	Mean	SD
Initial tumor volume (cm ³)	632.75	728.46	344.05	17.84	2655.02	620.65	828.49	382.79	14.98	5270.72	622.39	811.53
Follow-up tumor volume (cm ³)	1486.47	1967.63	749.19	102.70	8005.79	256.76	452.86	135.91	1.64	3438.86	454.12	943.35
Volume percentage change (%)	226.60	262.14	127.46	22.47	1,027.55	-58.12	30.88	-68.84	-99.76	11.19	-17.06	142.33

SD, standard deviation.

Tumor volumes and volume percentage changes after treatment in the progressive group were significantly larger than those before treatment, however, tumor volumes and volume percentage changes after treatment in the non-progressive group were significantly smaller than those before treatment (all $p < 0.01$)

*S.D.=Standard deviation (\pm), cm³ = Cubic centimeter.

- Regarding the quantitative analysis of DWI, we generated the ADC map, and then we selected the ROI manually. Most of the cases underwent three different ROIs centered upon the most restricted area in DWIs.
- The ADC value was automatically calculated on the workstation to get minimum and mean ADC values ($\times 10^{-3}$ mm).
- This method thought to be the less biased one giving an accurate assessment of the ADC value and mostly assess whole tumor volume.
- Measurements were recorded as a representative value for each case. Initial and follow-up images were matched and ADC calculations were performed on follow-up MRI.

Interpretation of dynamic contrast images:

- 21 out of 104 patients underwent DCE MRI.
- DCE images were done with quantitative analysis including ROI within different areas especially the suspicious restricted areas in DWIs.
- Time-signal intensity curve [TIC] with semi-quantitative (parameters derived from changes in the signal intensity) assessment identify the types of curve profile: progressive enhancement, delayed plateau, or delayed washout; type I, II, or III, respectively.
- The type of the curve with its quantitative parameters has been studied and correlated with the tumor necrosis since it indirectly reflects the vascularity of the tumor and indicates the viability of the tumor.

Statistical analysis

- (1) Statistical analysis was performed using the statistical software: SPSS statistical package v. 21 (SPSS Inc., Chicago, IL).
- (2) Numerical data were expressed as mean and standard deviation or median and range as appropriate. Qualitative data were expressed as frequency and percentage.
- (3) ROC analysis (receiver operator characteristic) was carried out to select the best cutoff point for ADC variations (ADC%).
- (4) The findings on initial MRI were analyzed and correlated with follow-up post-treatment MRI examinations and with post-operative histopathological findings when available.
- (5) MRI features that were analyzed included the location, tumor longest dimension based on (RECIST 1.1) at baseline and post neoadjuvant follow-up MRI examination referred to as RECENT 1 and RECENT 2 respectively. Similarly, the longest dimension of the contrast-enhanced portion of the tumor according to (m-RECIST) at baseline and follow-up MRI examination referred to as m-RECIST 1 and m-RECIST 2 respectively, the volume of the tumor before and after neoadjuvant therapy referred to as VOL1 and VOL2 respectively, signal characteristics and enhancement patterns.
- (6) Differences in tumor volumes (VOL%) was calculated as:

$$\text{VOL}\% = \frac{\text{VOL 2} - \text{VOL 1}}{\text{VOL 1}} \times 100$$

Similarly, RECIST % change calculated as:

Table 3. Quantitative DWI and ADC mapping was carried out for 102 cases of osteosarcoma and Ewing's sarcoma with detailed analysis of ADC(mm²/s) before and after neoadjuvant treatment values

Difference between initial and follow-up quantitative DWI values for 102 patients								
		Mean	SD (+/-)	Median	Minimum	Maximum	Mean difference	p-value
Osteosarcoma(51 patients)	Initial (minimum ADC)	0.71	0.24	0.65	0.35	1.60	0.51765	<0.001
	Follow-up (minimum ADC)	1.23	0.43	1.20	0.39	2.10		
	Initial (mean ADC)	0.90	0.29	0.86	0.50	2.20	0.71353	<0.001
	Follow-up (mean ADC)	1.62	0.46	1.64	0.60	2.70		
Ewing's sarcoma/PENT(51 patients)	Initial (minimum ADC)	0.42	0.19	0.40	0.07	0.85	0.65500	<0.001
	Follow-up (minimum ADC)	1.07	0.31	1.05	0.34	1.70		
	Initial (mean ADC)	0.71	0.16	0.70	0.50	1.00	0.90000	<0.001
	Follow-up (mean ADC)	1.60	0.39	1.70	0.57	2.30		
Mean ADC percentage change (%) for osteosarcoma		89.98	62.99	100.00	-50.00	215.07		0.001
Mean ADC percentage change (%) for Ewing's sarcoma/PENT		139.16	75.61	147.11	-36.67	260.00		

ADC, apparent diffusion coefficient; DWI, diffusion-weighted imaging.

$$\text{RECIST \%} = \frac{\text{RECIST 2} - \text{RECIST 1}}{\text{RECIST 1}} \times 100$$

m-RECIST% changes calculated as:

$$\text{mRECIST \%} = \frac{\text{mRECIST 2} - \text{mRECIST 1}}{\text{mRECIST 1}} \times 100$$

And ADC% changes calculated as:

$$\text{ADC \%} = \frac{\text{ADC 2} - \text{ADC 1}}{\text{ADC 1}} \times 100.$$

Each was calculated and statistically correlated.

- (7) Mean ADC values are selected for statistical analysis and compared with other MRI radiological findings and histopathological results when available.
- (8) The results were correlated with the postoperative pathology in 42 patients who underwent surgery. They were examined and grossly mapped systematically to determine the percentage of tumor necrosis. According to the histopathological examination, the effect of chemotherapy is assessed by two experienced pathologists based on the presence and extent of tumor necrosis. The necrosis is graded as grade I if 0–49%, grade II if 50–89%, grade III if 90–99%, and grade IV if 100% necrosis is detected. The effectiveness of chemotherapy was defined as “favorable or positive response” (≥90% tumor necrosis) or “adverse or negative response”

(<90% tumor necrosis). These patients were classified into two groups: favorable or positive responders (necrosis more than or equal to 90 %) and adverse or negative responders (necrosis less than 90 %).⁷

Statistical methods

Data were coded and entered using the statistical package SPSS (Statistical Package for the Social Science; SPSS Inc., Chicago, IL) v. 22. Data were summarized using mean, standard deviation, median, minimum, and maximum in quantitative data and using frequency (count) and relative frequency (percentage) for categorical data. Standard diagnostic indices including sensitivity, specificity, positive predictive value (PPV), negative predictive value (NPV), and diagnostic efficacy were calculated. ROC curve was constructed with an area under curve analysis performed to detect the best cutoff value of ADC for the detection of residue. For comparing categorical data, Chi-square (χ^2) test was performed. A *p*-value of less than 0.05 was considered statistically significant.

RESULTS

The patient's data including histopathological diagnoses and sites of the primary tumor were demonstrated in "Table 1".

Treatment response

Follow-up was conducted to evaluate the therapeutic response evaluation criteria in solid tumors (RECIST 1.1), (m-RECIST), and volume assessment. As regards the volume change; out of 104 patients, 11 (10.6%) patients had disease progression (PD) (increase in maximum tumor diameter > 20%), 52 (50%) patients showed stable disease (SD) (change in maximum tumor diameter between PR and progressive disease), and 41 (39.4%) patients had partial response (PR) (the decrease in maximum tumor diameter > 30) "Figure 1".

For statistical analysis, the patients were distributed into two groups: the PD group includes 11/104 of patients (10.6%) and the non-PD group including (PR + SD) 93/104 of patients (89.4%), according to the detection results "Figure 2".

MRI imaging features

Variations in tumor volumes and ADC values among both progressive and non-progressive groups are demonstrated in (Tables 2 and 3)", respectively.

Correlation between ADC values and tumor volumes before and after neoadjuvant treatment is demonstrated in "Table 4".

The ADC values after neoadjuvant treatment were negatively related to different tumor response parameters after neoadjuvant treatment with a statistically significant p -value ($p < 0.005$).

Radiological Response Evaluation" Table 5"

Based on RECIST 1.1 (the change in tumor longest dimension)

A decrease in tumor size based on RECIST is associated with an increase in ADC values after neoadjuvant therapy and vice versa. The Pearson correlation coefficient of tumor volumes and ADC values variations was $r = -0.427$ ($p < 0.001$) "Figure 3".

Based on m-RECIST

A decrease in tumor size based on m-RECIST is associated with an increase in ADC value after neoadjuvant therapy and vice versa. The Pearson correlation coefficient of differences in tumor sizes and ADC values was $r = -0.498$ ($p < 0.001$).

Based on tumor volume (VOL)

A decrease in tumor volume is associated with an increase in ADC value and vice versa. The Pearson correlation coefficient of differences in tumor volumes and ADC values was $r = -0.408$ ($p < 0.001$).

ROC curves showed that the areas under the curve (AUC) of the change of ADC values (ADC%) after neoadjuvant treatment was 0.807; the mean percentage of ADC% cut-off to differentiate PD and non-PD was 10.5% (sensitivity 60% and specificity 97.7%) "Table 6".

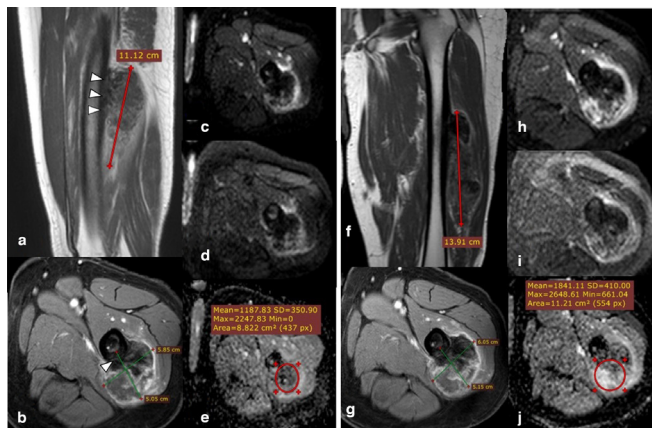
Hence, differences in tumor responses as assessed by RECIST, m-RECIST, and 3D volumetric measurements were directly correlated to each other, regardless of the effectiveness of anti-cancer therapy Figure 4, Table 7

Table 4. Detailed analysis of mean ADC values and ADC% change among both progressive and non-progressive groups

Difference between initial and follow-up quantitative DWI values for 102 patients		Mean	SD (+/-)	Median	Minimum	Maximum	Mean difference	p-value
Osteosarcoma (51 patients)	Initial (minimum ADC)	0.71	0.24	0.65	0.35	1.60	0.51765	<0.001
	Follow-up (minimum ADC)	1.23	0.43	1.20	0.39	2.10		
	Initial (mean ADC)	0.90	0.29	0.86	0.50	2.20	0.71353	<0.001
	Follow-up (mean ADC)	1.62	0.46	1.64	0.60	2.70		
Ewing's sarcoma/PENT (51 patients)	Initial (minimum ADC)	0.42	0.19	0.40	0.07	0.85	0.65500	<0.001
	Follow-up (minimum ADC)	1.07	0.31	1.05	0.34	1.70		
	Initial (mean ADC)	0.71	0.16	0.70	0.50	1.00	0.90000	<0.001
	Follow-up (mean ADC)	1.60	0.39	1.70	0.57	2.30		
Mean ADC percentage change (%) for osteosarcoma		89.98	62.99	100.00	-50.00	215.07		0.001
Mean ADC percentage change (%) for Ewing's sarcoma/PENT		139.16	75.61	147.11	-36.67	260.00		

ADC, apparent diffusion coefficient; DWI, diffusion-weighted imaging.

Figure 3. 30-year-old male with left femoral bone osteosarcoma juxta-cortical type (initial and follow-up MRI studies done). Post-contrast sagittal T1 & axial T1 fat-saturation (A, B) showing left femoral midshaft juxta-cortical heterogeneous enhancing lesion with focal cortical expansion/periosteal reaction (Arrowheads) and eccentric extra osseous soft tissue component with internal areas of persistently low signal (osteoid matrix/reaction), the calculated volume was 165.88 CC. DWI (b0 & b-800) images (C, D) show heterogenous signal with persistent internal areas of low signal corresponding to the osteoid matrix; which induce artifact at ADC map (E) with calculated values showing a minimum value of $0.0 \times 10^{-3} \text{ mm}^2/\text{s}$ while the mean value equals $1.1 \times 10^{-3} \text{ mm}^2/\text{s}$. Follow-up MRI assessment: Post-contrast coronal T1 & axial T1 fat-saturation (F, G) showing a minimal increase in size and volume of the lesion, with a calculated volume of 221 CC. follow-up markers of treatment response (RESIST, m-RESIST, and volume % changes) showing no appreciable change since the last study denoting stable disease. DWI (b0 & b-800) images (H, I) as well as ADC mapping (J) showing an increase in ADC values (mean: $2.15 \times 10^{-3} \text{ mm}^2/\text{s}$ and minimum: $1.7 \times 10^{-3} \text{ mm}^2/\text{s}$), yet the ADC % change is not significant to indicate a good therapeutic response. The post-operative histopathological assessment revealed poor therapeutic response with viable tumoral cells represents about 45% of the tumor volume, which matches follow-up parameters and DWI, yet DWI and ADC mapping can detect post-therapeutic subtle minor changes in tumor composition even if it is not still obviously noted in the morphology. ADC, apparent diffusion coefficient; DWI, diffusion-weighted imaging.



42 out of the 104 patients were a candidate for surgery and had a histological evaluation of the surgical specimens as regards the chemotherapeutic response.

All tumor specimens were examined by two experienced pathologists to determine the percentage of tumor necrosis. The effectiveness of chemotherapy was defined as “good” ($\geq 90\%$ tumor necrosis) or “poor” ($< 90\%$ tumor necrosis). Therefore, the lesions were divided into the following **two groups**: Group A ($n = 21$) included the cases with $\geq 90\%$ tumor necrosis after chemotherapy, and Group B ($n = 21$) included the cases with $< 90\%$ tumor necrosis "Table 8"& "Figure 5".

Figure 4. 11-year-old female presented with left leg extra skeletal Ewing sarcoma/PNET (initial and follow-up MRI studies done). Post-contrast sagittal T1 (A) and post-contrast axial T1 fat saturation (B) showing left mid-leg extra osseous intensely enhancing soft tissue mass lesion is seen eccentrically encasing the mid tibial shaft. No evidence of cortical erosion or intra medullary infiltrative lesions, with a calculated volume of 33.9 CC. DWI (b-0 & b-800) images (C, D) as well as ADC map (E) showing restricted signal with calculated ADC values of (mean: $0.62 \times 10^{-3} \text{ mm}^2/\text{s}$ and minimum: $0.42 \times 10^{-3} \text{ mm}^2/\text{s}$). Follow-up MRI: Post-contrast coronal T1 & axial T1 fat-saturation (F, G) showing notable regressive course of the size and volume with a calculated volume of 2.8 CC. DWI (b-0 & b-800) images (H, I) as well as ADC mapping (J) show facilitated signal (ROI with mean value of: $1.5 \times 10^{-3} \text{ mm}^2/\text{s}$ and minimum: $1.2 \times 10^{-3} \text{ mm}^2/\text{s}$). The post-operative histopathological assessment revealed a good therapeutic response with no viable tumoral tissue in the excised lesion, matches the DWI & ADC mapping as well as the RESIST and volume % changes. ADC, apparent diffusion coefficient; DWI, diffusion-weighted imaging.

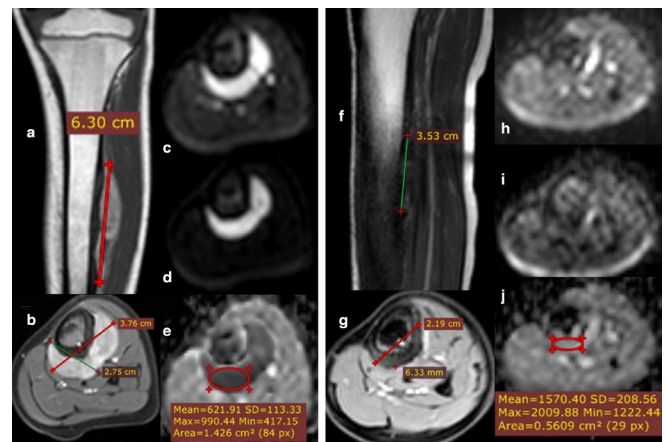


Table 5. Correlation between the different radiological evaluation percentage of change and ADC percentage of change

		Percentage (mean ADC change) (%)
Volume percentage change (%)	Pearson correlation	-0.408-
	p-value	<0.001
	N	101
Diameter (RECIST) percentage change (%)	Pearson correlation	-0.427-
	p-value	<0.001
	N	101
Modified RECIST percentage change (%)	Pearson correlation	-0.498-
	p-value	<0.001
	N	101

ADC, apparent diffusion coefficient.

Table 6. ADC variation values (ADC%) in detecting the efficacy of neoadjuvant treatment in Ewing's sarcoma and osteosarcoma

Area under the curve	p-value	95% Confidence Interval		Cut-off	Sensitivity %	Specificity %
		Lower bound	Upper bound			
0.807	<0.001	0.661	0.953	10.5335	60	97.7

Mean ADC and minimum ADC the difference between the pre- and post-chemotherapy ADC values, as well as mean and minimum ADC % changes, were compared in each group (Group A and Group B).

The mean ADC % in Group A and Group B was 119.33 ± 41.61 and 58.96 ± 60.44 (mean \pm SD) respectively. The minimum ADC % in Group A and Group B were 138.15 ± 66.99 and 45.79 ± 63.37 respectively. There was a statistically significant difference between Group A and Group B being more evident with minimum ADC % (p -value < 0.001) "Table 9" & "Figure 6".

DCE-MR imaging

21 patients pathologically proved osteosarcoma (16) and ES (5) underwent DCE-MRI. The initial dynamic contrast curves of 21 patients of osteosarcoma and ES showing about 18 patients (85.7%) of patients initially presented with Type III washout curve while the remaining 3 patients (14.3%) showing a Type II plateau curve. Post-treatment DCE-MRI sequence for those 21 patients was carried out and showed 11 patients (52.4%) with Type I continuous raising curve while the other 47.6% had Type III washout curve and Type II plateau curve by equal percent of 5 patients (23.8%) each. Based on the changes in the TIC on post-therapy DCE-MRI studies; patients divided into responsive (10 patients) and non-responsive (11 patients).

DCE quantitative parameters for the non-responsive patients were statistically calculated and correlated with the histopathological response "Table 10". The significance of each parameter was calculated and illustrated in "Table 11".

The patients were all candidates for surgery and each of them had a histological evaluation of the surgical specimens as with regards to the chemotherapeutic response.

Based on histopathological tumor therapy assessment, cases were divided into the following two groups: Group A ($n = 11$) included the cases with $\geq 90\%$ tumor necrosis after chemotherapy and Group B ($n = 10$) included the cases with $< 90\%$ tumor necrosis.

Correlation with the post-operative histopathological response assessment with calculated specificity and sensitivity for the DCE-MRI sequence revealed a sensitivity of about 100% and specificity of 81.82% (Table 12).

The cut-off criteria of $\leq 100\%$ max relative enhancement were predictive of favorable response with 90% sensitivity, 100% specificity, and 0.973 AUC. While the relative enhancement of \leq

20%, had 100% sensitivity, 81.8% specificity, and 0.923 AUC, in predicting favorable response' (Tables 13 and 14)'.

Max enhancement of $\leq 1000\%$, had sensitivity 80%, specificity 90.9% and AUC of 0.855%, wash-in rate ≤ 22.7 L/s. also predicted favorable response with 90% sensitivity, 81.8% specificity, and

Figure 5. 17-year-old male presented with right femoral Ewing's sarcoma (initial and follow-up MRI studies done). Post-contrast sequences (sagittal T1 & axial T1 fat saturation) (A, B) showing left distal femoral heterogeneous enhancing destructive mass lesion extends to the knee articular surface showing predominantly internal areas of breakdown. The calculated volume of the lesion was 3099.84 CC. DWI (b-0 & b-800) images (C, D) with ADC map (E) showing heterogeneous restricted signal with calculated ADC values of (mean: $0.89 \times 10^{-3} \text{ mm}^2/\text{s}$ and minimum: $0.34 \times 10^{-3} \text{ mm}^2/\text{s}$). Follow-up MRI assessment: Post-contrast coronal T1 & axial T1 fat saturation (F, G) showing: progression of the size/volume and extension of the lesion with a calculated volume of 8469.14 CC with increased internal breakdown. The markers of treatment response (RESIST and volume % changes) indicates progressive disease while (m-RESIST) showing stable disease. ADC mapping (H) also showing an increase in mean ADC values (mean: $1.1 \times 10^{-3} \text{ mm}^2/\text{s}$) while mean ADC values still stationary (minimum: $0.36 \times 10^{-3} \text{ mm}^2/\text{s}$), the minimal value suggest viable restricted tumoral tissue. The patient underwent palliative operation with post-operative histopathological assessment revealed poor therapeutic response with viable tumoral cells represents about 70% of the tumor volume. Post-therapeutic effect with tumoral break down can increase the tumor size so m-RESIST has a great role as it depends upon the measurement of viable enhancing component, carrying a high risk of human error while DWI & ADC make proper mapping of areas of restriction (active tumor tissue presented by minimum ADC value) and facilitation (areas of break down) with quantitative values decrease the risk of bias. ADC, apparent diffusion coefficient; DWI, diffusion-weighted imaging.

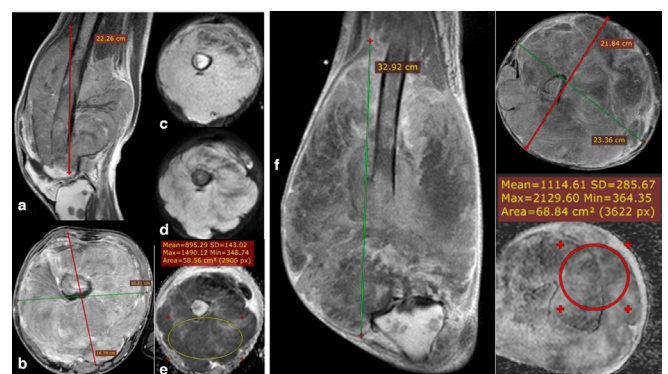


Table 7. Accuracy measures of RECIST 1.1 and m-RECIST in correlation to the volume as a gold standard

		Volume group				p-value
		Progressive disease		Non-progressive disease		
		Count	%	Count	%	
Diameter (RECIST) group	Progressive disease	10	66.7%	1	1.1%	<0.001
	Non-progressive disease	5	33.3%	88	98.9%	
Modified RECIST group	Progressive disease	6	40.0%	1	1.1%	<0.001

0.845 AUC. Washout rate of ≤ 5 L/s suggested favorable response with 100% sensitivity, 45.45% specificity and 0.755 AUC.

DISCUSSION

Recent guideline for the management of osteosarcoma and ES depends mainly upon MRI to monitor the treatment efficacy, response, surgical planning and determine the patient's prognostic factors.^{4,6,8}

Several authors have shown the importance of DWI with ADC apparent diffusion coefficient mapping to assess post-treatment response in osteosarcoma and Ewing's sarcoma.⁹

The gold-standard for judging the curative effect of chemotherapy is tumor necrosis rate using a histological method, but this method is traumatic due to repeated biopsy.¹⁰

DWI and ADC changes are inversely related to tumor cellularity⁹ and are currently considered a non-invasive measure of the local diffusion characteristics of water molecules *in vivo*.^{10,11}

Also DCE-MR imaging is a promising method of physiologic imaging that has been applied to osteosarcoma and ES. It provides clinically useful information by depicting tissue vascularization and perfusion.¹² Viable tumor tissue exhibits a characteristic rapid uptake and a large accumulation of contrast media, while necrotic tumor tissue enhances less rapidly and less intensely.¹³

In this study, tumor morphologic changes post-neo-adjuvant therapy (based on RECIST 1.1, m-RECIST, and three-dimensional volumetric assessments) were statistically analyzed and turned out to be positively correlated to each other. Different studies use volumetric measurements in the assessment of the tumor response especially soft tissue sarcomas and correlated with ADC

values and ADC ratios. Koh et al, le Grange et al., Messiou et al, and Soldatos et al.'s studies didn't perform volumetric measurements in their studies, the only maximum dimension of each mass was assessed, and ADC values were assessed after completion of neoadjuvant therapy only with no baseline pretreatment MRI assessment.^{11,14-16}

Wang et al.'s study revealed that in contrast to the measurement of tumor size and volume, ADC-measurements were shown to be superior to monitor treatment efficacy.¹⁰

Contrarily, this study showed that the pre-therapy ADC values in the progressive group showed no difference from those in the non-progressive group. In support of our results, DeVries et al.'s study highlighted the potential pitfall of using mean tumor ADC values for prognostication in 34 rectal cancer patients undergoing chemo-radiation. They showed no differences between mean pretreatment ADC in the 18 patients who responded and the 16 patients who were non-responders.¹⁷

Different studies underwent pre-treatment quantitative ADC map assessment in cases of osteosarcoma and ES, yet no definite gold-standard values of each tumor. Costa et al and Pekcevik et al.'s studies described that ES showed the lower ADC value compared to osteosarcoma and other tumors as it is a member of small round blue cell tumors with compacted cellular structure, while osteosarcoma is a spindle cell tumor.^{18,19}

This study revealed that the mean pre-treatment ADC values of osteosarcoma and Ewing's sarcoma were $(0.90 \pm 0.29$ and $0.71 \pm 0.16)$ mm²/s respectively.

In this study, one of the major limitations was that the post-surgical pathological response as a gold standard is not available in more than half of the patients. To overcome this limitation, we use

Table 8. Detailed pathological response in each osteosarcoma and Ewing's sarcoma

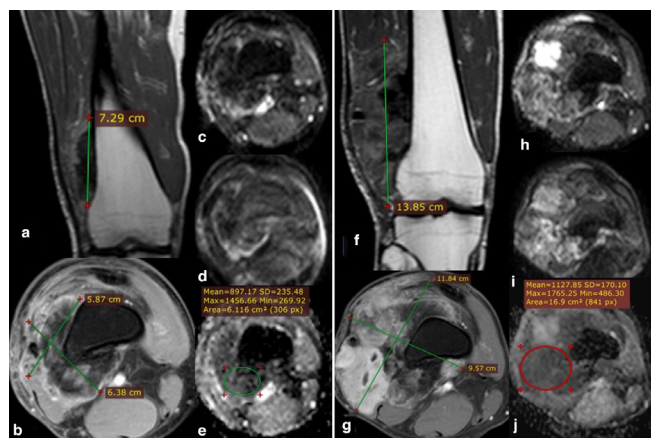
Necrosis (%)	Osteosarcoma		Ewing's sarcoma		Total
	Frequency	Percentage (%)	Frequency	Percentage (%)	
Good response ($\geq 90\%$ tumor necrosis)	14/29	48.3%	7/13	53.8%	21
Poor response ($< 90\%$ tumor necrosis)	15/29	51.7%	6/13	46.2%	21
Total	29	100%	13	100%	42

Table 9. Detailed analytical values of ADC (mm²/s) of 42 cases of osteosarcoma and Ewing's sarcoma with correlation to postoperative pathological response

	Pathological response											p-value
	Good response (≥90% tumor necrosis)					Poor response (<90% tumor necrosis)						
	Mean	SD	Median	Minimum	Maximum	Mean	SD	Median	Minimum	Maximum		
Initial minimum ADC (x 10 ³ mm ² /s)	0.57	0.14	0.56	0.23	0.85	0.79	0.30	0.70	0.40	1.60		0.006
Initial mean ADC (x 10 ³ mm ² /s)	0.79	0.14	0.76	0.60	1.00	1.00	0.39	0.88	0.68	2.20		0.032
Follow-up minimum ADC (x 10 ³ mm ² /s)	1.32	0.36	1.20	0.80	2.10	1.06	0.37	1.00	0.45	1.90		0.041
Follow-up mean ADC (x 10 ³ mm ² /s)	1.72	0.31	1.70	1.12	2.30	1.48	0.50	1.40	0.60	2.70		0.044
Mean ADC variation (%)	119.33	41.61	117.91	46.07	215.07	58.96	60.44	64.71	-50.00	179.41		0.001
Minimum ADC variation (%)	138.15	66.99	130.77	33.33	272.09	45.79	63.37	28.57	-34.78	200.00		<0.001

ADC, apparent diffusion coefficient.
 Note: **There was a statistically significant difference between Group A and Group B being more evident with minimum ADC % (p-value < 0.001).**
 aSD=Standard deviation (±)

Figure 6. 37-year-old male with right femoral osteosarcoma juxta-cortical type (initial and follow-up MRI studies done). Post-contrast coronal T1 & axial T1 fat-saturation (A, B) showing distal femoral juxta-cortical heterogeneously enhancing mass lesion showing predominantly internal areas of persistent low signal (osteoid matrix) with a calculated volume of 144.55 CC. No evidence of sizable intra medullary infiltrative lesions. DWI (b-0 & b-800) images (C, D) show heterogeneous signal with persistent internal areas of low signal corresponding to the osteoid matrix; which induces artifact at ADC map (E) with calculated values of (mean: 0.89 × 10⁻³mm²/s and minimum: 0.269 × 10⁻³mm²/s). Follow-up MRI: Post-contrast sequences (coronal T1 & axial T1 fat saturation) (F, G) showing progression of the size/volume and extension of the lesion with a calculated volume of 749.19 CC. Follow-up markers of treatment response (RESIST, m-RESIST, and volume % changes) indicates progressive disease. DWI (b-0 & b-800) images (H, I) as well as ADC mapping (J) showing mild increase in ADC values (mean: 1.1 × 10⁻³mm²/s and minimum: 0.48 × 10⁻³mm²/s), yet the ADC % change is not significantly indicates good therapeutic response. The post-operative histopathological assessment revealed poor therapeutic response with viable tumoral cells represents about 80% of the tumor volume, which matches follow-up the size/volume percentage changes even with minimal increase in quantitative ADC values. So the morphological and size of the lesion is a cornerstone parameter in follow-up assessment before proceeding to DWIs and ADC mapping. ADC, apparent diffusion coefficient; DWI, diffusion-weighted imaging.



tumor morphologic changes post-neoadjuvant therapy (based on RECSIT 1.1, m-RECIST, and three-dimensional volumetric assessments) and dividing patients into two groups; progressive and non-progressive groups.

The ADC values and ADC parentage change (ADC%) after neoadjuvant treatment in the non-progressive group were significantly higher than those before neoadjuvant treatment (1.69 ± 0.33 vs 1.16 ± 0.62) with (p 0.001).

In this study, ADC variations (ADC%) in the non-progressive group were significantly higher than those of the progressive group (128.30 ± 63.49 vs -36.34 ± 78.73) % with (p < 0.001). That is comparable to the work of Wang et al.'s study who investigated the role of DWI in monitoring the therapeutic response

Table 10. Detailed quantitative parameters of the TIC of 21 patients at initial and follow-up DCE-MRI assessment with follow-up patients categorization into responsive and non- responsive groups

			Relative enhancement %	Maximum enhancement %	Maximum relative enhancement %	Time to peak (s)	Washin rate (L/s)	Washout rate (L/s)
Parameters of Initial TIC for 21 patients		Mean	25.96	1343.957	112.564	139.2643	44.232	9.381
		Minimum	0	50.52	5.81	23.2200	7.77	0
		Maximum	104.86	4214.01	257.40	329.4500	186.45	58.92
		SD	33.511	1090.157	79.055	102.5662	57.977	16.40
Parameters of follow-up TIC for 21 patients	Non-responsive 11 patients	Mean	46.69	1770.96	172.217	73.82	70.588	16.063
		Minimum	0	829.77	110.55	23.22	7.77	0.89
		Maximum	104.86	3012.00	275.40	180.8	186.45	58.92
		SD	34.86	722.45	45.814	39.49	70.879	20.78
	Responsive 10 patients	Mean	3.165	874.25	46.94	211.25	15.24	2.031
		Minimum	0	50.52	5.81	50	8.36	0
		Maximum	20	4214.01	150	329.4	41.76	5.00
		SD	6.529	1262.16	49.21	103.2	10.23	1.895

SD, standard deviation; TIC, time-intensity curve.

^aSD=Standard deviation, S. = second, L = Liter

Table 11. Correlation between the quantitative parameters of the time-intensity curve of responsive and non- responsive groups along with the follow-up DCE-MRI of 21 patients

	TIC for 11 non-responsive patients		TIC for 10 responsive patients		p-values
	Mean	S.D.	Mean	S.D.	
Relative enhancement %	46.69	34.86	3.165	6.529	0.001
Maximum enhancement %	1770.96	722.45	874.25	1262.16	0.006
Maximum relative enhancement %	172.217	45.814	46.94	49.21	0.002
Time to peak (s)	73.82	39.49	211.25	103.2	0.006
Washin rate (L/s)	70.588	70.879	15.24	10.23	0.0066
Washout rate (L/s)	16.063	20.78	2.031	1.895	0.047

DCE, dynamic contrast enhancement; TIC, time-intensity curve.

after neoadjuvant chemotherapy in osteosarcoma of long bones in 34 patients found that in patients with good response, the

post-neoadjuvant chemotherapy values were significantly higher than the pre-neoadjuvant chemotherapy values.¹⁰

Table 12. Correlation between the post-operative histopathological response and DCE-MRI response type

	Value	95% CI
Sensitivity	100.00%	69.15 to 100.00%
Specificity	81.82%	48.22 to 97.72%
Positive likelihood ratio	5.50	1.57 to 19.27
Disease prevalence (*)	47.62%	25.71 to 70.22%
Positive predictive value (*)	83.33%	58.80 to 94.60%
Negative predictive value (*)	100.00%	
Accuracy (*)	90.48%	69.62 to 98.83%

DCE, dynamic contrast enhancement.

Our results were also supported by the work of Baunin et al.'s study on patients diagnosed with osteosarcoma and found that good responders had a significantly higher ADC variation (ADC%) than poor responders (38.3 ± 15.09 vs 12.02 ± 22.9) however, the ADC differential (ADC2-ADC1) of the tumor was also calculated in these cases.²⁰

The comparison of ADC results between different series expressed as absolute ADC values remains difficult. The main reason is the use of different MR techniques and settings. One way to standardize the results is to use ADC differentials (ADC2-ADC1) or variations (ADC %). ADC variations (ADC %) in percentage terms should be more reproducible and could

Table 13. Correlation between the different radiological evaluation response parameters and response change in DCE-MRI images

		Response change in DCE-MRI images (responsive and non-responsive)
Volume change (progressive and non-progressive)	Pearson correlation	0.730
	<i>p</i> -value	0.0002
	N	21
Diameter (RECIST) change (progressive and non-progressive)	Pearson correlation	0.560
	<i>p</i> -value	0.0083
	N	21
Modified RECIST change (progressive and non-progressive)	Pearson correlation	0.645
	<i>p</i> -value	0.0016
	N	21

DCE, dynamic contrast enhancement.

also be more easily understood by clinicians for comparison to histological response.^{20,21}

In our series, ADC variations (ADC%) were inversely correlated with morphologic changes, regardless of the effectiveness of anticancer therapy expressed as changes of tumor size based on (RECIST, m-RECIST and three-dimensional volumetric assessment), Linear regression analysis revealed a Pearson correlation coefficient of $r = (-0.427, -0.498 \text{ and } -0.408)$ respectively with ($p < 0.001$). This relationship was independent of the neoadjuvant therapy protocol or length of the treatment period, although treatment regimens and imaging intervals were too heterogeneous for statistical analysis.

This is comparable to the study done by Dudeck et al.'s study in which variations in ADC (ADC%) were inversely correlated with changes of tumor volumes (VOL%) with yet had a stronger Pearson correlation coefficient; $r = -0.925$ ($p < 0.0001$).²²

Unlike Dudeck et al.'s study, our study revealed that an increase in the ADC value was not always associated with a reduction of tumor volume. Likewise, a decrease in ADC was not always associated with an increase in tumor volume in all patients.²²

In this study, 42 patients underwent post-operative histopathological response evaluation, calculating the tumor necrosis

percentage of the excised lesions. The effectiveness of chemotherapy is considered to be good if more than 90% tumor necrosis is observed.

There was a direct relationship between treatment-induced elevation of ADC values and the extent of tumor necrosis. This matched to similar studies done.^{10,21}

In this study, the minimum and mean ADC values with ADC % of each were used to assess tumor response with a significant difference was demonstrated between the patients with a good response to chemotherapy and those with a poor response. The significant differences were obvious and strong mainly with minimum ADC values and minimum ADC%.

This matched the study done by Oka et al.'s study which revealed a significant difference between the good and poor responders among the minimum ADC values, but the study revealed that; no statistically significant difference was observed in the mean ADC ratio.²¹

Since the cellularity of osteosarcomas is heterogeneous, especially post-chemotherapy, the variations in the ADC values are large. For this reason, so the study presumed that the areas with the highest cellularity within heterogeneous tumors best reflect

Table 14. Cut-off values of different quantitative parameters of the time-intensity curve along with the follow-up DCE-MRI of 21 patients with ROC curves

DCE-parameters	Cut-off value	AUC	Sensitivity (%)	Specificity (%)	Confidence interval
Maximum enhancement %	≤ 1000	0.855	80	90.91	0.633–0.968
Maximum relative enhancement %	≤ 100	0.973	90	100	0.793–1
Relative enhancement %	≤ 20	0.923	100	81.82	0.72–0.993
Time to peak (s)	> 123.22	0.755	80	81.82	0.52–0.913
Washin rate (L/s)	≤ 22.7	0.845	90	81.82	0.623–0.964
Washout rate (L/s)	≤ 5	0.755	100	45.45	0.52–0.913

AUC, area under the curve; DCE, dynamic contrast-enhanced; ROC, receiver operating characteristic.

the characteristics of the tumors and best assessed by minimum ADC values.

Degnan et al.'s study revealed that the mean ADC was the single-best predictor of treatment status for pediatric bone tumors. This finding likely reflects the greater statistical robustness of a mean ADC value compared with minimum values, which may be more prone to measurement error.⁴

According to these results, the calculation of an ADC value seems to be a promising quantitative and sensitive surrogate to monitor response to chemotherapy in osteosarcomas and ES.

This study used a DCE-MRI semi-quantitative assessment in the form of TIC. ROIs put on different tumoral areas in initial and follow-up studies with TIC either Type I continuous rising curve, Type II plateau curve and Type III washout curve.^{13,23}

Quantitative assessment using software with multiple parameters were used on our studies like maximum relative enhancement (%), time to peak (s), washin, and washout rates (mL/s). Assessment of the treatment response in this study used the change in the curve shape as well as different raw parameters like the maximum relative enhancement (%), time to peak (s), wash-in and washout rates (mL/s).^{6,23}

The study revealed that most of the patients (85.7%) presented at initial MRI study with a Type III malignant washout curve which nearly matched the results of Fayad et al.'s and Cao et al.'s studies.^{13,24}

The responsive cases in the study showed the change in the TIC all represented with Type I continuous rising curve. This matched Sujlana et al.'s study who revealed that good treatment response can present as a decrease in size of the lesion or formation of macroscopic necrosis and fibrosis/scarring which presented in static postcontrast images with heterogeneous enhancement and DCE curve showing slowly over time enhancement in comparison to rapidly enhancing residual tumor.²³

Also, it matched other studies were using the slope of the curve in assessment of the treatment response, like Murphy et al.'s and Sujlana et al.'s studies which revealed that a reduction in the curve slope value after chemotherapy by more than 60% was considered a favorable response.^{3,23}

The non-responsive patients presented with different types of curve changes with the majority showed type II and III curves. This is matching the results of Amit et al.'s and Kubo et al.'s studies which showed a high curve slope in the post-treatment viable tumors denoting adverse response.^{1,5}

Correlation between the changes in the curve shape followed post-chemo- or radiotherapy compared to the post-operative histopathological response revealed a positive correlation with a sensitivity of about 100% and specificity of 81.8%. This was nearly similar to Amit et al.'s study which showed a correlation of clinical and MRI response with the histologic response, as defined by tumor necrosis and correlated between percentage change in curve slope and histopathological tumor necrosis.^{5,12}

Although the sample size in our study is large, yet we had some limitations first, treatment response assessment was based on RECIST 1.1. as not all patients were candidates for surgery and our results were not correlated to post-operative histopathological response results in all cases. A second limitation of tumor volume was calculated by simple mathematical formulas. An irregular shape might not fit well into an ellipsoidal or cylindrical formula, and there is a risk of over- or underestimation of tumor volume.

CONCLUSION

A multiparametric radiologic approach is needed for evaluation of treatment response in malignant bone tumors, since it is unlikely that a single radiologic parameter alone can allow prediction of treatment response in tumors.

Serial assessment of quantitative diffusion changes in tumors with different chemotherapy and radiation therapy treatment protocols could serve as a novel indicator of treatment response and aid in more rational decision-making regarding treatment approaches in cases of osteosarcoma and ES.

AUTHORS CONTRIBUTIONS

AM wrote the manuscript and is responsible for correspondence to journal. MS collected patient data, image processing and collection of patients images. TM participated in the design of the study and performed the statistical analysis. GM was responsible of pathological data. AS conceived of the study, and participated in its design and coordination and helped to draft the manuscript. YM was responsible of revision of the draft from clinical point of view.

PATIENT CONSENT

All patients included in this research gave written informed consent to publish the data contained within this study.

ETHICS APPROVAL AND CONSENT TO PARTICIPATE

The study was approved by the institutional review board (IRB) of the National Cancer Institute, Cairo university with ethical committee approval number 201617060.3, session 120 and approval date 15/5/2018. An informed written consent was taken from all subjects.

REFERENCES

- Kubo T, Furuta T, Johan MP, Adachi N, Ochi M. Percent slope analysis of dynamic magnetic resonance imaging for assessment of chemotherapy response of osteosarcoma or Ewing sarcoma: systematic review and meta-analysis. *Skeletal Radiol* 2016; **45**: 1235–42.
- Toguchida J. (eds) Genetics of Osteosarcoma. In: *Osteosarcoma*. Tokyo: Springer; 2016. pp. 3–17. doi: <https://doi.org/10.1002/jmri.21358>
- Murphey MD, Senchak LT, Mambalam PK, Logie CI, Klassen-Fischer MK, Kransdorf MJ. From the radiologic pathology Archives: Ewing sarcoma family of tumors: radiologic-pathologic correlation. *Radiographics* 2013; **33**: 803–31.
- Degnan AJ, Chung CY, Shah AJ. Quantitative diffusion-weighted magnetic resonance imaging assessment of chemotherapy treatment response of pediatric osteosarcoma and Ewing sarcoma malignant bone tumors. *Clin Imaging* 2018; **47**: 9–13.
- Amit P, Patro DK, Basu D, Elangovan S, Parathasarathy V. Role of dynamic MRI and clinical assessment in predicting histologic response to neoadjuvant chemotherapy in bone sarcomas. *Am J Clin Oncol* 2014; **37**: 384–90.
- Vilanova JC, Baleato-Gonzalez S, Romero MJ, Carrascoso-Arranz J, Luna A. Assessment of musculoskeletal malignancies with functional MR imaging. vol. 24, magnetic resonance imaging clinics of North America. *W.B. Saunders* 2016;: 239–59.
- Picci P, Bacci G, Campanacci M, Gasparini M, Pilotti S, Cerasoli S, et al. Histologic evaluation of necrosis in osteosarcoma induced by chemotherapy. regional mapping of viable and nonviable tumor. *Cancer* 1985; **56**: 1515–21.
- Redondo A, Bagué S, Bernabeu D, Ortiz-Cruz E, Valverde C, Alvarez R, et al. Malignant bone tumors (other than Ewing's): clinical practice guidelines for diagnosis, treatment and follow-up by Spanish group for research on sarcomas (GEIS. *Cancer Chemother Pharmacol* 2017; **80**: 1113–31.
- Kubo T, Furuta T, Johan MP, Ochi M, Adachi N. Value of diffusion-weighted imaging for evaluating chemotherapy response in osteosarcoma: a meta-analysis. *Mol Clin Oncol* 2017; **7**: 88–92.
- Wang C-S, Du L-J, Si M-J, Yin Q-H, Chen L, Shu M, et al. Noninvasive assessment of response to neoadjuvant chemotherapy in osteosarcoma of long bones with diffusion-weighted imaging: an initial in vivo study. *PLoS One* 2013; **8**: e72679. doi: <https://doi.org/10.1371/journal.pone.0072679>
- Messiou C, Bonvalot S, Gronchi A, Vanel D, Meyer M, Robinson P. Evaluation of response after pre-operative radiotherapy in soft tissue sarcomas. *the European Organisation for Research and Treatment of Cancer – Soft Tissue and Bone Sarcoma Group (EORTC – STBSG) and Imaging Group recommendations for radiological examina* 2016; **56**: 37–44.
- Amit P, Malhotra A, Kumar R, Kumar L, Patro DK, Elangovan S. Evaluation of static and dynamic MRI for assessing response of bone sarcomas to preoperative chemotherapy: correlation with histological necrosis. *Indian J Radiol Imaging* 2015; **25**: 269–75.
- Cao J, Xiao L, He B, Zhang G, Dong J, Wu Y, et al. Diagnostic value of combined diffusion-weighted imaging with dynamic contrast enhancement MRI in differentiating malignant from benign bone lesions. *Clin Radiol* 2017; **72**: 793.e1–793.e9.
- Koh D-M, Blackledge M, Collins DJ, Padhani AR, Wallace T, Wilton B, et al. Reproducibility and changes in the apparent diffusion coefficients of solid tumours treated with combretastatin A4 phosphate and bevacizumab in a two-centre phase I clinical trial. *Eur Radiol* 2009; **19**: 2728–38.
- le Grange F, Cassoni AM, Seddon BM. Tumour volume changes following pre-operative radiotherapy in borderline resectable limb and trunk soft tissue sarcoma. *Eur J Surg Oncol* 2014; **40**: 394–401.
- Soldatos T, Ahlawat S, Montgomery E, Chalian M, Jacobs MA, Fayad LM. Multiparametric assessment of treatment response in high-grade soft-tissue sarcomas with anatomic and functional MR imaging sequences. *Radiology* 2016; **278**: 831–40.
- DeVries AF, Kremser C, Hein PA, Griebel J, Krezcy A, Öfner D, et al. Tumor microcirculation and diffusion predict therapy outcome for primary rectal carcinoma. *Int J Radiat Oncol Biol Phys* 2003; **56**: 958–65.
- Costa FM, Ferreira EC, Vianna EM. Diffusion-Weighted magnetic resonance imaging for the evaluation of musculoskeletal tumors. *Magn Reson Imaging Clin N Am* 2011; **19**: 159–80.
- Pekcevik Y, Kahya MO, Kaya A. Diffusion-Weighted magnetic resonance imaging in the diagnosis of bone tumors: preliminary results. *J Clin Imaging Sci* 2013; **3**: 63.
- Baunin C, Schmidt G, Baumstarck K, Bouvier C, Gentet JC, Aschero A, et al. Value of diffusion-weighted images in differentiating mid-course responders to chemotherapy for osteosarcoma compared to the histological response: preliminary results. *Skeletal Radiol* 2012; **41**: 1141–9.
- Oka K, Yakushiji T, Sato H, Hirai T, Yamashita Y, Mizuta H. The value of diffusion-weighted imaging for monitoring the chemotherapeutic response of osteosarcoma: a comparison between average apparent diffusion coefficient and minimum apparent diffusion coefficient. *Skeletal Radiol* 2010; **39**: 141–6.
- Dudeck O, Zeile M, Pink D, Pech M, Tunn P-U, Reichardt P, et al. Diffusion-Weighted magnetic resonance imaging allows monitoring of anticancer treatment effects in patients with soft-tissue sarcomas. *J Magn Reson Imaging* 2008; **27**: 1109–13.
- Sujlana P, Skrok J, Fayad LM. Review of dynamic contrast-enhanced MRI: technical aspects and applications in the musculoskeletal system. *J Magn Reson Imaging* 2018; **47**: 875–90.
- Fayad LM, Jacobs MA, Wang X, Carrino JA, Bluemke DA. Musculoskeletal tumors: how to use anatomic, functional, and metabolic Mr techniques. *Radiology* 2012; **265**: 340–56.